Phase diagram of binary Ti-Ni alloys on Ti-rich side under a pressure of 2.2 GPa

H. ARAKI, T. YAMANE*, M. NAKANO
Department of Materials Science and Engineering, Osaka University, 2-1 Yamada-oka, Suita, Osaka 565-0871, Japan
E-mail: yamane2@h6.dion.ne.jp

Y. MINAMINO
Department of Adaptive Machine System, Osaka University, 2-1 Yamada-oka, Suita, Osaka 565-0871, Japan

---

Pressure is a variable whereby the state of an alloy can be determined independent of temperature and composition. Researchers [1–5] have shown that application of hydrostatic pressure of the order of GPa can change phase equilibria in metallic systems and thus increase maximum solubilities and induce eutectoid and peritectoid reactions that do not occur at ambient pressure. The ability to exploit high pressure to fabricate novel, superior materials, which cannot be produced under ambient pressure, relies on the establishment of high-pressure phase equilibria.

The ambient pressure phase diagram for the binary Ti-Ni alloy has been established [6], while the alloy's high pressure phase diagram has yet to be determined. The present authors have experimentally established the Ti-rich part of the phase diagram at 2.2 GPa through measurements of Ni concentrations at phase boundaries in two phase alloys and diffusion couples annealed at the hydrostatic high pressure.

A Ti bar (99.79 mass%Ti, impurity: C 80, N 70, O 1300, H 6 ppm, respectively) was rolled into a plate at room temperature, polished with emery paper and cut into pieces. To produce Ti-Ni alloys, Ni pellets (99.97 mass%Ni, Co 0.5, Cu 1, Fe 15, S 3, C 100 ppm, respectively) were ultrasonically cleaned in acetone and arc-melted several times with appropriate amounts of Ti in high purity Ar atmosphere. The solidified Ti-Ni ingots contained 3.00, 4.87, 7.41, 11.81, 15.06, 33.63 and 39.68 at%Ni. These ingots were homogenized at 1173 K for 604.8 ks in Ar gas. The homogenized Ti-15.06 at%Ni alloy contained 1600 ppm O and 40 ppm N by mass, which was virtually identical to the oxygen and nitrogen content of the original Ti bar.

The Ti bar and the homogenized Ti-Ni alloys were cut into blocks about 2 mm in thickness and about 3–5 mm^2 in cross-section, after which joint surfaces were polished with a series of emery papers and finally buffed with 0.05 μm alumina powders. Several Ti, Ti-15.06 at%Ni and Ti-39.68 at%Ni blocks were clamped in stainless steel jigs to be used as a diffusion couple in an experiment at ambient pressure. The alloys and diffusion couples were annealed at various diffusion annealing temperatures in silica tubes evacuated and back-filled with Ar (0.1 MPa). Ti-7.41 and Ti-15.06 at%Ni blocks were annealed for 0.9 ks at 1273 K and for 14 ks at 1423 K respectively, and Ti/Ti-15.06 at%Ni and Ti/Ti-39.68 at%Ni diffusion couples were done for 3.6 to 172.8 ks at temperatures from 1023 to 1198 K.

For the high-pressure experiment, the Ti bar and Ti-Ni alloys were lathed and cut into cylinders 4 mm in diameter and 2.5 or 5 mm in height. Their surfaces were metallographically polished as described above. A Ti cylinder was coupled with a Ti-Ni alloy cylinder (2.5 in mm height) to form a diffusion couple. All high pressure anneals of alloys and couples were performed under 2.2 GPa, in the high pressure cells shown in Fig. 1, in the same manner as reported in more detail [7–9]. Under a 2.2 GPa hydrostatic pressure generated by a cubic anvil apparatus, Ti-11.81 and 15.06 at%Ni alloys were annealed for 0.6 to 1.8 ks at temperatures from 1263 to 1423 K, and Ti/Ti-15.06 at%Ni and Ti/Ti-39.68 at%Ni diffusion couples were done for 3.6 to 28.8 ks at temperatures from 1013 to 1248 K. The high pressure annealed specimens were cooled faster than 50 K/s during the first 10 s. The Ti-Ni alloys and diffusion couples annealed under 0.1 MPa and 2.2 GPa were cut and embedded in resin, and then metallographically polished with emery paper and 0.05 μm alumina powder. Intensities of the characteristic X-ray of Ni K_α were measured with an electron probe microanalyzer and converted to

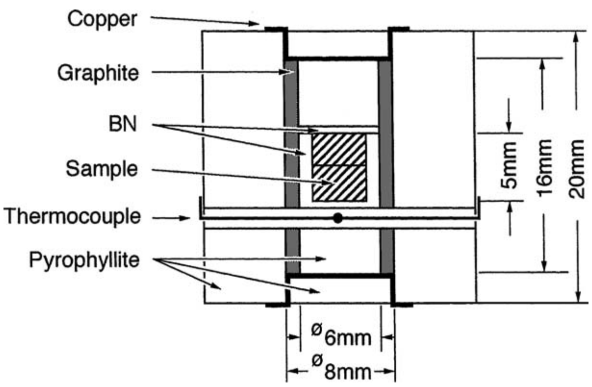

Figure 1 High pressure cell. A sample was equally pressed from its vertical six directions and subjected to hydrostatic high pressure.

Present address: 1-9-12-1005 Imazu-minami, Tsurumi-ku, Osaka 538-0043, Japan.

TABLE I Phase boundary concentrations in Ti/Ti-15.06 at%Ni diffusion couple annealed for various time at 1123 K and 0.1 MPa

Diffusion time (ks)	αTi + βTi/βTi phase boundary concentration (at%Ni)	βTi/βTi + Ti$_2$Ni phase boundary concentration (at%Ni)	
	Diffusion profile	Diffusion profile	Concentration in βTi phase
3.6	3.38	7.61	7.72
14.4	2.83	7.53	7.55
115.2	3.12	7.73	7.75

Ni concentrations by comparing to the characteristic peaks of Ti-3.00, 4.87, 7.41, and 33.64 at%Ni single phase alloys rapidly cooled from 1223 K using the following equation proposed by Ziebold and Ogilvie [10, 11]:

$$(1 - X)/X = K(1 - I)/I \qquad (1)$$

$$I = (I_{\text{measured}} - I_0)/(I_{\text{Ni}} - I_0) \qquad (2)$$

where, X is the Ni mass fraction composition of Ni, K a constant and I the relative intensity of Ni K$_\alpha$ radiation. I_{measured} is the measured Ni K$_\alpha$ intensity of a sample, I_{Ni} the intensity of pure Ni, and I_0 the background intensity. In the present experiment, K was 1.007.

It is very important to confirm that the Ni concentrations at phase boundaries are independent of the annealing time. Tables I and II show the Ni concentrations at the phase boundaries of αTi + βTi/βTi and βTi/βTi + Ti$_2$Ni in the Ti/Ti-15.06 at%Ni couple annealed for various times at 1123 K under 0.1 MPa and 2.2 GPa, respectively. In the Ti-15.06 at%Ni alloy, the βTi and Ti$_2$Ni phases co-exist at the annealing temperature under 0.1 MPa and 2.2 GPa, and the βTi/βTi + Ti$_2$Ni phase boundary concentrations were thus obtained both from the diffusion profiles in the vicinity of the joint interfaces between pure Ti and Ti-15.06 at% Ni alloy, and from the concentrations of βTi phases equilibrated with Ti$_2$Ni phases in the central parts of Ti-15.06 at%Ni alloys. The two results are in good agreement, as shown in Tables I and II. The phase boundary concentrations are solely dependent on the pressure, and independent of diffusion time. Thus, the authors established the Ti-Ni phase diagrams by measurement of Ni concentration in annealed diffusion couples and two-phase alloys. Moreover, Tables I and II show that the βTi phase region is expanded by the application of 2.2 GPa because the Ni concentration of the βTi/βTi + Ti$_2$Ni phase boundary is raised by the high pressure, whereas that of the αTi + βTi/βTi phase boundary is lowered.

TABLE II Phase boundary concentrations in Ti/Ti-15.06 at%Ni diffusion couple annealed for various time at 1123 K and 2.2 GPa

Diffusion time (ks)	αTi + βTi/βTi phase boundary concentration (at%Ni)	βTi/βTi + Ti$_2$Ni phase boundary concentration (at%Ni)	
	Diffusion profile	Diffusion profile	Concentration in βTi phase
7.2	2.47	8.67	8.80
14.4	2.88	8.10	8.14
28.8	2.78	8.05	8.20

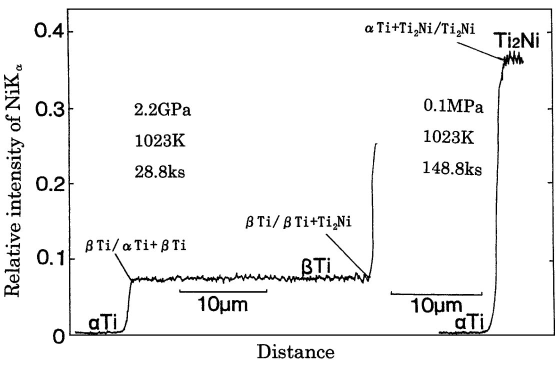

Figure 2 Diffusion profiles in Ti/Ti-15.06 at%Ni couple annealed for 148.8 ks at 1023 K and 0.1 MPa, and for 28.8 ks at 1023 K and 2.2 GPa.

Fig. 2 shows the diffusion profiles in the Ti/Ti-15.06 at%Ni couples both annealed at 1023 K, one under 0.1 MPa, the other under 2.2 GPa. The βTi layer forms at 2.2 GPa; it is not observed at 0.1 MPa where the annealing temperature of 1023 K is lower than the temperature of the eutectoid reaction βTi $\rightarrow$ αTi + Ti$_2$Ni. This means that the βTi phase is relatively stabilized by the application of 2.2 GPa and the eutectoid reaction is shifted to the lower temperature.

As seen in Fig. 2, the diffusion rates of Ni and Ti atoms are much lower in αTi and Ti$_2$Ni phases than in βTi phase. Hence, the diffusion distances are correspondingly shorter in the former two phases. The diffusion distances in αTi and Ti$_2$Ni phases are very short in the annealed diffusion couples, and the αTi and Ti$_2$Ni phases occur in very low quantities in the equilibrated alloys. Thus, the present work focuses on the αTi/αTi + βTi and βTi/βTi + Ti$_2$Ni phase boundary concentrations.

Fig. 3 shows the Ti-rich part of the binary phase diagrams at 0.1 MPa and 2.2 GPa obtained in this

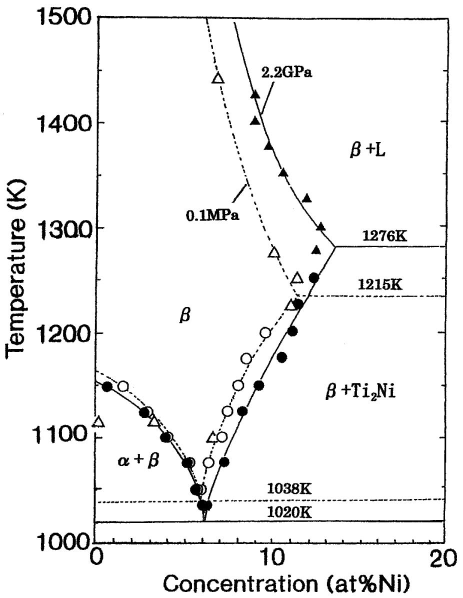

Figure 3 Phase diagrams of binary Ti-Ni alloys at 0.1 MPa and 2.2 GPa: (△), Two phase alloy annealed at 0.1 MPa; (▲), Two phase alloy annealed at 2.2 GPa; (○), Diffusion couple annealed at 0.1 MP; (●), Diffusion couple annealed at 2.2 GPa.

work. The application of the high pressure (2.2 GPa) shifts the αTi + βTi/βTi and βTi/βTi + Ti_2Ni phase boundaries to the Ti- and Ni-rich sides by about 0.2 and 1 at%Ni, respectively. The βTi region is thus expanded. Based on the αTi + βTi/βTi and βTi/βTi + Ti_2Ni phase boundaries determined in this work, the eutectoid point is extrapolated to be at 6 at%Ni and 1020 K under 2.2 GPa. Its Ni content is nearly equal to that obtained under 0.1 MPa in the present study, which is higher than the value reported by Murray (4.5 at%Ni) [6]. The estimated eutectoid temperature at 2.2 GPa is 18 K lower than that at 0.1 MPa obtained in this work, which is equal to that determined by Murray [6]. The application of 2.2 GPa raises the solidus line by about 50 K. The point of intersection of solidus line and βTi/βTi + Ti_2Ni phase boundary line suggest that the eutectic temperature and the maximum solubility are 1276 K and 13.5 at%Ni at 2.2 GPa respectively. The estimated temperature is 61 K higher than the eutectc temperature at 0.1 MPa (1215 K) [6]. The maximum solubility at 2.2 GPa is also higher than that at 0.1 MPa (13 at%Ni) [6]. These results indicate that high pressure treatment enables us to get single βTi phase alloys containing over 10 at%Ni, which do not exist in the equilibrium state at 0.1 MPa.

References

1. R. E. HANNEMAN, R. E. OGILVIE and H. C. GATOS, *Trans. Met. Soc. AIME* **233** (1965) 685.
2. Y. MINAMINO, T. YAMANE, H. ARAKI, A. HIRAKI and Y. MIYAMOTO, *J. Iron Steel Inst. Jpn.* **74** (1988) 733.
3. Y. MINAMINO, T. YAMANE, H. ARAKI, T. ADACHI and Y. S. KANG, *J. Mater. Sci.* **26** (1991) 5623.
4. H. ARAKI, Y. MINAMINO, T. YAMANE, K. AZUMA, Y. S. KANG and Y. MIYAMOTO, *J. Mater. Sci. Lett.* **11** (1992) 181.
5. T. YAMANE, Y. S. KANG, Y. MINAMINO, H. ARAKI, A. HIRAKI and Y. MIYAMOTO, *Z. Metallkd.* **86** (1995) 453.
6. J. L. MURRAY, "Binary Alloy Phase Diagrams," 2nd ed., Editor in Chief, T. B. Massalski (ASM International, Metals Park, Ohio 44073, USA, 1990) Vol. 3, p. 2874.
7. T. TAKAHASHI, T. YAMANE, T. YAMAMOTO, H. ARAKI, Y. MINAMINO and Y. MIYAMOTO, *Z. Metallkd.* **85** (1994) 492.
8. H. ARAKI, S. SAJI, T. OKABE, Y. MINAMINO, T. YAMANE and Y. MIYAMOTO, *Mater. Trans. JIM* **38** (1997) 247.
9. T. YAMANE, K. HISAYUKI, K. YOSHIDA, Y. MINAMINO, H. ARAKI and K. HIRAO, *J. Mater. Sci.* **34** (1999) 1835.
10. T. O. ZIEBOLD and R. E. OGILVIE, *Anal. Chem.* **36** (1964) 322.
11. G. F. BASTIN and G. D. RIECK, *Metall. Trans.* **5** (1974) 1817.

Received 11 December 2003
and accepted 23 June 2004